frontiers | Frontiers in Marine Science

TYPE Original Research
PUBLISHED 26 October 2022
DOI 10.3389/fmars.2022.1002398

OPEN ACCESS

EDITED BY
Gilles Reverdin,
Centre National de la Recherche Scientifique (CNRS), France

REVIEWED BY
Peter Landschützer,
Max Planck Institute for Meteorology, Max Planck Society, Germany
Amanda Fay,
Columbia University, United States

*CORRESPONDENCE
Di Qi
qidi@jmu.edu.cn

SPECIALTY SECTION
This article was submitted to Marine Biogeochemistry, a section of the journal Frontiers in Marine Science

RECEIVED 25 July 2022
ACCEPTED 11 October 2022
PUBLISHED 26 October 2022

CITATION
Wu Y and Qi D (2022) Inconsistency between ship- and Argo float-based pCO_2 at the intense upwelling region of the Drake Passage, Southern Ocean. *Front. Mar. Sci.* 9:1002398. doi: 10.3389/fmars.2022.1002398

Inconsistency between ship- and Argo float-based pCO_2 at the intense upwelling region of the Drake Passage, Southern Ocean

Yingxu Wu[1,2] and Di Qi[1]*

[1]Polar and Marine Research Institute, Jimei University, Xiamen, China, [2]Ocean and Earth Science, National Oceanography Centre Southampton, University of Southampton, Southampton, United Kingdom

The Southern Ocean absorbs a quarter of anthropogenic carbon dioxide (CO_2) from the atmosphere to modulate the climate system. However, less attention has been paid to the CO_2 outgassing phenomenon at the Antarctic Circumpolar Current (ACC) region of the Southern Ocean due to strong upwelling. Recent studies using autonomous biogeochemical-Argo float revealed a greater winter CO_2 outgassing than previously estimated at ACC zone of the Southern Ocean, which, however, remains controversial and urgently needs to be validated. Here we take the Drake Passage as a case study to present new insights into the Southern Ocean carbon cycle and examine the validity of float-based CO_2 outgassing. Upon integrating the ship-based data over the past two decades, we investigate the spatiotemporal variability of sea surface CO_2 partial pressure (pCO_2) in Drake Passage. We show that Drake Passage is acting as a year-round weak CO_2 sink, although some CO_2 uptake is counteracted by winter CO_2 outgassing. The float-based pCO_2 values are overall higher than ship-based values in winter, by 6 to 20 µatm (averaged 14 µatm) at the most intensive upwelling region. We then develop a surface carbon balance calculation (considering mixing between surface, subsurface, and upwelled waters) to estimate the potential of surface pCO_2 increase due to upwelling, and we find that upwelling of CO_2-rich subsurface waters in Drake Passage cannot support an excess ΔpCO_2 of 14 µatm as suggested by float detections. We further compare our results to previous study and find that, although we used same datasets and obtained comparable results, the way to conclude the bias in float-based pCO_2 would cause significant difference: an uncertainty of ±2.7% (i.e., ± 11 µatm) in float-based pCO_2 estimated by other study seems acceptable, however, it is five times larger than the typical ship-based pCO_2 uncertainty (± 2 µatm), and

would cause ~180% bias in CO_2 flux estimates. Going forward, there is special need for caution when interpreting the float-based CO_2 flux; meanwhile, further comparisons and corrections between float- and ship-based pCO_2 are clearly warranted.

KEYWORDS

CO_2 partial pressure, upwelling, CO_2 outgassing, Drake Passage, Southern Ocean

1 Introduction

The Southern Ocean plays an outsized role in the global carbon cycle and therefore regulating the global climate system (Sarmiento & Toggweiler, 1984; Gruber et al., 2019a; Gruber et al., 2019b). The Southern Ocean (south of 30°S) is responsible for a disproportionately large percentage (~40%) of the total oceanic sink of anthropogenic CO_2 (Mikaloff Fletcher et al., 2006; Gruber et al., 2009; DeVries, 2014; Gruber et al., 2019a; Gruber et al., 2019b), as well as the large-scale control of nutrient supplies to the low-latitude oceans and therefore the magnitude of low-latitude biological productivity (Sarmiento et al., 2004). Observations and models have demonstrated large variability in the efficiency of uptake of CO_2 in the Southern Ocean over the past few decades. The strength of the Southern Ocean CO_2 sink was reported to have slackened from the 1980s to the early 2000s due to the increase in Southern Ocean winds which enhances the upwelling and outgassing of natural CO_2 (Le Quéré et al., 2007; Lovenduski et al., 2008). In contrast, recent studies (Landschützer et al., 2015; Munro et al., 2015b) suggest reinvigoration of the Southern Ocean CO_2 uptake since 2002, due to the cooling in the Pacific Ocean, enhanced stratification in the Atlantic and Indian Ocean sectors, and a reduced overturning (Landschützer et al., 2015; DeVries et al., 2017; Gruber et al., 2019b).

The Southern Ocean is uniquely important due in large part to its circulation. Deep waters from both the Atlantic and the Indo-Pacific are upwelled to the surface, and then transformed into intermediate waters or denser bottom waters (Lumpkin & Speer, 2007; Marshall & Speer, 2012; Talley, 2013). The upwelling mostly occurs at the southern portion of the Antarctic Circumpolar Current (ACC) (Orsi et al., 1995; Thorpe et al., 2002; Chapman et al., 2020), where deep waters return to the upper ocean *via* wind-driven Ekman transport (Marshall & Speer, 2012) and release the remineralized CO_2 that has been accumulated and isolated from the atmosphere over centuries. Such CO_2 release is concentrated to a relatively narrow band between 50°S and 65°S (Chen et al., 2022). Previous studies (e.g., Wu et al., 2019) have demonstrated a strong latitudinal gradient in surface dissolved inorganic carbon (DIC), where DIC is highest in the high-latitude Southern Ocean as a consequence of low temperature and upwelling; and high-DIC subsurface waters outcrop along the upwelling pathway. However, this might not be identical to the partial pressure of CO_2 (pCO_2, which fundamentally matters to air-sea CO_2 exchange) given that pCO_2 is also regulated by the excess total alkalinity (TA), seawater temperature and salinity, resulting in a distinct vertical distribution of pCO_2 (Chen et al., 2022). Therefore, a more comprehensive understanding of the upwelling impacts on surface pCO_2 is required to decipher the mechanism of upwelling-induced deep CO_2 release.

Despite its vital impact on the carbon cycle and climate system, the Southern Ocean remains one of the most poorly sampled regions of the global ocean and characterized by large uncertainty in CO_2 flux estimates (Bakker et al., 2016; Gruber et al., 2019b; Friedlingstein et al., 2022). The Drake Passage is, however, an exception with a lot of high-frequency and high-resolution observational data made since 2002 as part of the Drake Passage Time-series Project. The carbon cycle and carbonate system in Drake Passage is consequently better understood (Munro et al., 2015a; Munro et al., 2015b; Fay et al., 2018) than elsewhere in the Southern Ocean, and suggested to be representative of a broader region in the subpolar Southern Ocean in both seasonality and long-term CO_2 trends.

With the aim of filling data gaps and gaining better understandings of the Southern Ocean carbon cycle, starting since 2014, the Southern Ocean Carbon and Climate Observations and Modeling (SOCCOM) program has deployed the first biogeochemical float array across the Southern Ocean. More than 200 floats, equipped with oxygen, nitrate, pH, and bio-optical sensors (Johnson et al., 2017) have been released (https://soccom.princeton.edu/). The carbonate system data (e.g., pCO_2) were derived from the float-measured pH and algorithm-calculated TA. Based on the first several years of limited SOCCOM data, Williams et al. (2017); Gray et al. (2018) and Bushinsky et al. (2019) showed a surprisingly large CO_2 outgassing signal around the ACC zone, in particular in winter, at a much greater rate (0.36 Pg C $year^{-1}$) than previous ship-based estimates (from -0.05 to 0.03 Pg C $year^{-1}$; according

to Landschützer et al., 2014 and Takahashi et al., 2009). They attributed the increases in the carbon and nutrient content of surface waters in the high-latitude Southern Ocean primarily to the scarcity of pCO_2 observations prior to the float measurements being available as well as interannual variability, e.g., a positive Southern Ocean Annular Mode Index over 2014-2017 resulted in increased wind-driven upwelling (Lovenduski et al., 2007; Lovenduski et al., 2008). However, some recent evidences with independent approaches (e.g., airborne observations, uncrewed surface vehicle observations, reconstructions of winter data, and paired CO_2-O_2 metrics; Long et al., 2021; Mackay & Watson, 2021; Sutton et al., 2021; Wu et al., 2022) showed that the biogeochemical-Argo might have overestimated sea surface pCO_2, thus adding more controversy to the accurate estimates of CO_2 flux. The discrepancy between ship-based and float-based estimates of surface pCO_2 and air-sea exchange therefore motivated us to examine the validity of such strong CO_2 outgassing in the ACC zone of the Southern Ocean. For this purpose, we take advantage of the Drake Passage dataset and its representation of the subpolar Southern Ocean carbon cycle to investigate the ship-based seasonal variability of sea surface pCO_2. In order to gain a mechanistic understanding, we develop a surface carbon balance calculation (accounting for deep entrainment of CO_2 from subsurface water and upwelled water) to estimate the theoretical value of winter surface pCO_2 under the influence of vertical mixing and upwelling.

2 Materials and methods

2.1 Study area: Drake Passage

The strong flow of the zonally unbounded Antarctic Circumpolar Current (ACC) is constricted to as narrow as ~800 km, making Drake Passage a natural laboratory for investigating the entire ACC system over a relatively short distance (Sprintall et al., 2012). We followed the previous studies (Munro et al., 2015a; Munro et al., 2015b) to divide Drake Passage into four regions according to its unique physical oceanography and geographic settings. The four regions (Figure 1A) in Drake Passage are oriented parallel to the Antarctic Polar Front (APF) and the mean flow of the ACC, with two of them (R1 and R2) located north of the APF and the other two (R3 and R4) located south of the APF. The Subantarctic Front (SAF) locates within R1, the APF locates between R2 and R3.

2.2 Data source

We used several observational datasets containing surface pCO_2 and carbonate system parameters as described below. The austral summer is defined as from January to March, and so on for the other seasons.

2.2.1 The time-series data in Drake Passage

Discrete surface samples for parameters (e.g., salinity, macronutrients, and DIC) as well as high-frequency underway pCO_2 measurements were collected and measured on five to eight transects of Drake Passage per year by the Antarctic Research Supply Vessel *Laurence M. Gould*. The carbonate system parameters as well as other biogeochemical variables measured onboard (referred to as Drake Passage Time-series, DPT) allow for a comprehensive understanding of the biogeochemistry in Drake Passage. The DPT dataset during 2002 to 2017 (Figure 1A) was downloaded from https://www.ldeo.columbia.edu/res/pi/CO2/. The analytical precision was ±2 μatm for underway pCO_2, and approximately ±1 μmol kg^{-1} for DIC (Munro et al., 2015a; Munro et al., 2015b). TA was calculated from DIC, pCO_2, temperature, salinity, phosphate, and silicate data. The estimated accuracy of each TA value was 2 μmol kg^{-1} based on the analytical precision of pCO_2 and DIC (Takahashi et al., 2014; Munro et al., 2015a; Munro et al., 2015b). The computed TA values were relatively close to the measured TA values (of the samples with pCO_2, DIC, and TA measurements) by titration (root-mean-square deviation of ±4 μmol kg^{-1}).

We also took advantage of the existing water column profiles in Drake Passage in March 2006, February and September 2009 (Figure 1A). The data were obtained from the GLODAPv2.2020 dataset (Olsen et al., 2020), with uncertainties of 4 μmol kg^{-1} and 6 μmol kg^{-1} for DIC and TA, respectively.

2.2.2 SOCCOM float data

The SOCCOM Biogeochemical-Argo float data were downloaded from https://soccom.princeton.edu/, and 8 floats intersecting Drake Passage (from 2014 to 2020) were used in this study (Figure 1B). The float measures water column pH, oxygen, nitrate, fluorescence, and backscattering (Johnson et al., 2017). Carbonate system parameters including pCO_2 and others are first calculated from sensor-measured temperature, salinity, pH, LIAR algorithm-estimated TA, and silicate and phosphate concentrations (Williams et al., 2016; Williams et al., 2017; Carter et al., 2018). All float data were quality controlled as described in Johnson et al. (2017). Specifically, the quality control of pH data is based on the crossover analysis for deep waters between float and shipboard (including available Southern Ocean dataset and SOCCOM deployment cruises) measurements. The empirical algorithm for estimating in-situ pH as a function of temperature, salinity, pressure, and O_2 is determined for shipboard bottle measurements at 1000-2000 m depth, which is then applied to float-measured temperature, salinity, pressure, and O_2. By comparing the two pH values at 1500 m depth, an offset in pH is applied to the entire float profile. The measured pH has a reported uncertainty of 1% (equivalent

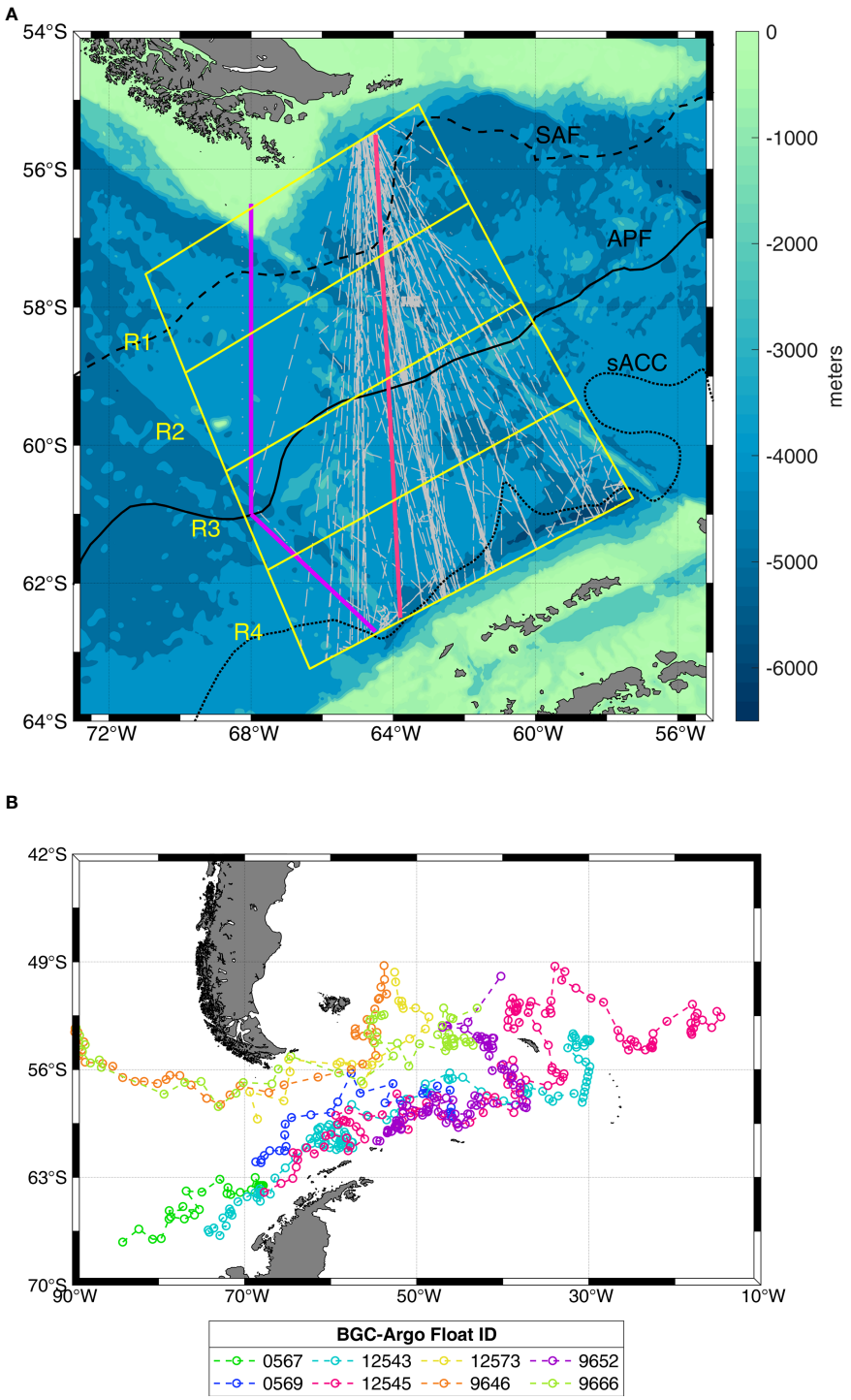

FIGURE 1
The observations from ship-based underway measurements and biogeochemical-Argo float in the Drake Passage. **(A)** underway pCO_2 measurements indicated by grey lines. The black dashed line indicates the location of SAF, black solid line indicates APF, and black dotted line indicates southern ACC front (front data obtained from Orsi et al., 1995; Thorpe et al., 2002). The cruises with water column sampling are denoted by purple and pink lines, in February 2009 and March 2006/September 2009, respectively. The coordinates of the box corners from the top corner of R1 to the bottom corner of R4 are: 55.06°S, 63.29°W; 57.52°S, 70.97°W; 56.49°S, 61.87°W; 58.95°S, 69.85°W; 57.92°S, 60.39°W; 60.38°S, 68.71°W; 59.34°S, 58.85°W; 61.81°S, 67.54°W; 60.77°S, 57.26°W; and 63.24°S, 66.35°W. **(B)** Argo floats that intersected the study area. Eight floats were selected.

to 0.005) respectively (Johnson et al., 2017), and the estimated TA and pCO_2 have a reported uncertainty of 5.6 μmol kg^{-1} and 2.7% respectively (Williams et al., 2017).

The uncertainty associated with the float-estimated pCO_2 mainly results from three factors: accuracy of the estimated TA, accuracy of the measured pH, and the choice of equilibrium constants used for calculating the carbonate system (Williams et al., 2017). Among them, the accuracy of the measured pH was proven to be the dominant factor (Williams et al., 2017; Takeshita et al., 2018). According to a quality control assessment through December 2016 (Johnson et al., 2017), the pH sensor was recorded to have the lowest percentage (88%) of good data return, while the oxygen sensor had the best percentage (100%) of good data return. Some previous efforts have been made to reveal the mismatch between float-based and ship-based pH values (Álvarez et al., 2020; Wu et al., 2022).

2.3 Data processing

2.3.1 Detrend of pCO_2

In order to prevent the temporal CO_2 trends from generating artificial spatial variability due to anthropogenic CO_2 influence, we detrended the surface pCO_2 and normalized it to a reference year 2005 for a better comparison with global studies (e.g., Takahashi et al., 2014). The rate of trend of 1.67 μatm yr^{-1} accounting for increasing atmospheric CO_2 during the 2002-2017 period was determined from the underway pCO_2 measurements used in this study (Figure 2A). The rate varies slightly across the particular region (R1-R4) in the Drake Passage, with deviations less than 0.23 μatm yr^{-1} (Figures 2B–E), which equals to 2.76 μatm bias for a 12-year normalization from 2005 to 2017. This is within the uncertainty of pCO_2 measurements and therefore could be negligible. We further applied this rate to the entire Drake Passage when normalizing the ship-based and float-based pCO_2 to 2005.

2.3.2 Surface carbon balance calculation

Figure 3 shows the seasonal changes in water mass properties in Drake Passage (Evans et al., 2014). In winter, a large amount of Antarctic Winter Water (AAWW) and Antarctic Intermediate Water (AAIW) are formed due primarily to strong surface cooling and consequent deep mixed layers, whilst in summer, AAWW is eroded through surface warming and interior mixing with surface water until the following winter. Compared to the surface water in either summer or winter, AAWW is supposed to exhibit increased salinity and DIC (Table 1). By quantifying the individual contributions of Summer Surface Water (SSW) and AAWW to the surface carbon balance in Winter Surface Water (WSW), we can then reach an estimate of how seasonal water mass transformation changes surface DIC and pCO_2.

Due to the fact that most of the float-observed strong CO_2 outgassing occurs in the ACC zone (Williams et al., 2017; Gray et al., 2018), we combined zone R3 and R4 (south of APF and north of southern ACC) in Drake Passage (Figure 1) to investigate the surface carbon balance. During the mixing of SSW and AAWW to form WSW, the fraction of AAWW (f_{AAWW}) was calculated as the amount necessary to change the surface concentration [X] of a specific tracer from its observed value at the beginning of the entrainment (i.e., summer months) period to the value at the end of the entrainment (i.e., winter months), according to Equations 1 and 2:

$$f_{SSW} + f_{AAWW} = 1 \quad (1)$$

$$([X]_{SSW} \times f_{SSW}) + ([X]_{AAWW} \times f_{AAWW}) = [X]_{WSW} \quad (2)$$

where $[X]_{SSW}$ is the concentration in Summer Surface Water, and $[X]_{WSW}$ is for Winter Surface Water. In addition, we also considered the mixture of Upper Circumpolar Deep Water (UCDW) and SSW to form WSW which is an extreme scenario that barely happens in the study area (Figure 3A). In this case the endmember AAWW was replaced by UCDW. Two conservative parameters, total alkalinity (TA) and absolute salinity (S_A), were chosen to quantify this process separately. The absolute salinity is defined as the mass fraction of salt in seawater as opposed to practical salinity which is essentially a measure of the conductivity of seawater to describe the salt content of seawater; absolute salinity is an SI unit of concentration with units of g kg^{-1}.

The AAWW water mass is defined by its characteristic ranges in absolute salinity and conservative temperature (T_{cons}), with S_A ranging from 34 g kg^{-1} to 34.3 g kg^{-1}, and T_{cons} ranging from -2°C to 1°C (Evans et al., 2014). The conservative temperature is a new standard for ocean temperature adopted by the oceanographic community as part of the Thermodynamic Equation of Seawater – 2010 (TOES-10), which is based on a hypothetical adiabatic and isohaline change in pressure to the sea surface. Table 1 summarizes the average values of the two tracers as well as the carbonate parameters in each mixing endmember; the values for AAWW and UCDW were taken from depth profile data, and the values for SSW and WSW were taken from the detrended surface underway data. The Gibbs-SeaWater Toolbox was used to calculate absolute salinity and conservative temperature.

Uncertainties for the calculated fractions of different water masses and the subsequent mixed DIC and pCO_2 were estimated from a 1000-iteration Monte Carlo analysis that contained uncertainties of each input parameters as listed in Table 1. The principle of Monte Carlo analysis follows Wu et al. (2019).

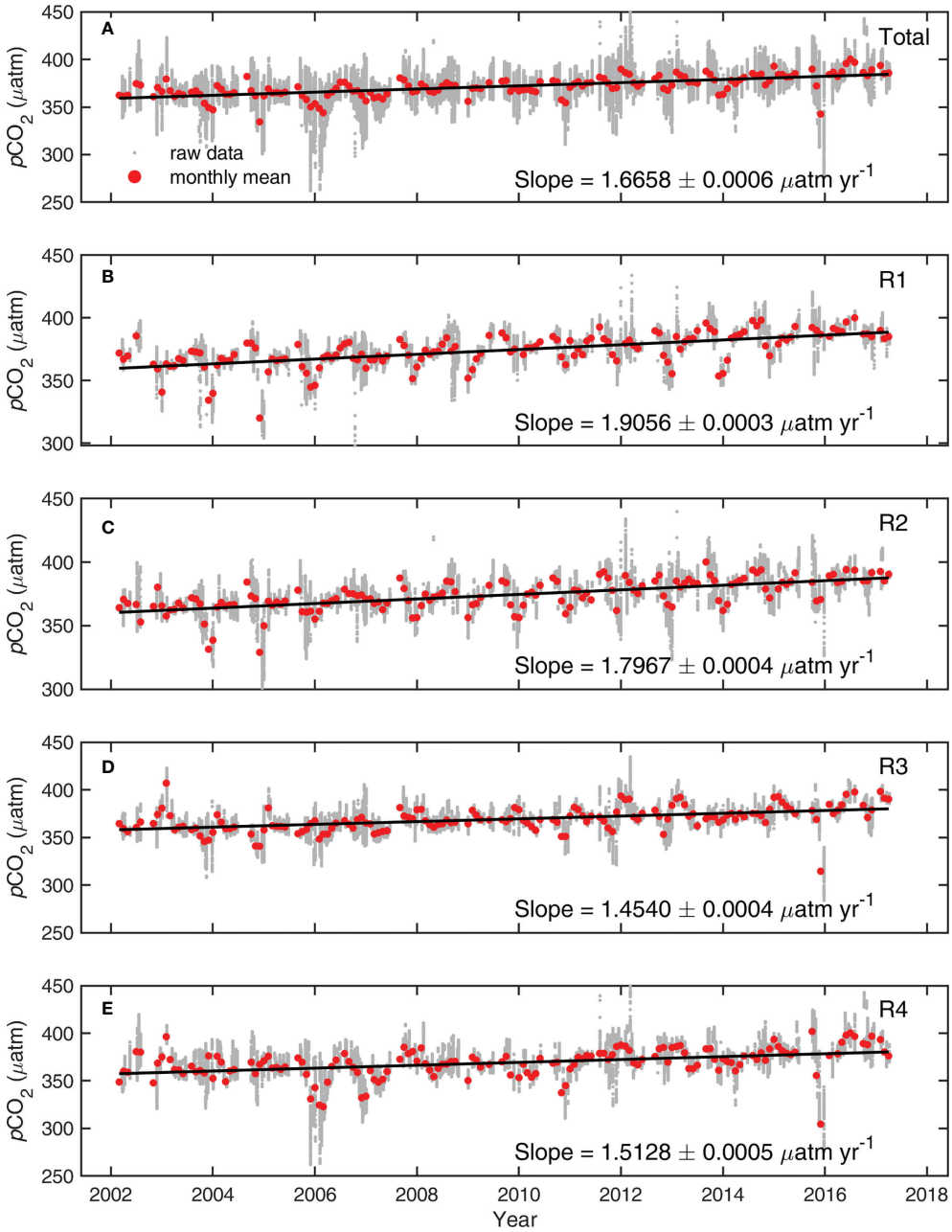

FIGURE 2
The inter-annual variation in surface pCO_2 in the Drake Passage **(A)** and specifically in its four regions **(B–E)** The grey dots are the raw pCO_2 data, the red dots are the monthly mean pCO_2 values. The slope of linear regression is used to detrend surface pCO_2.

3 Results

3.1 Spatiotemporal variability of ship-based surface pCO_2 in Drake Passage

The surface pCO_2 (normalized to reference year 2005) displayed distinct patterns in each season across the four regions in Drake Passage (Figure 4). Spatially, surface pCO_2 exhibit an overall decreasing trend against latitude in spring, autumn, and winter; however, became more dynamic in summer due to the possible interaction with biological activity (Brown et al., 2019). Noteworthy, a hotspot of high pCO_2 was found in R4 particularly in spring and winter, which is due to upwelling around ACC zone. The latitudinal gradient in pCO_2 was sizable in both summer and

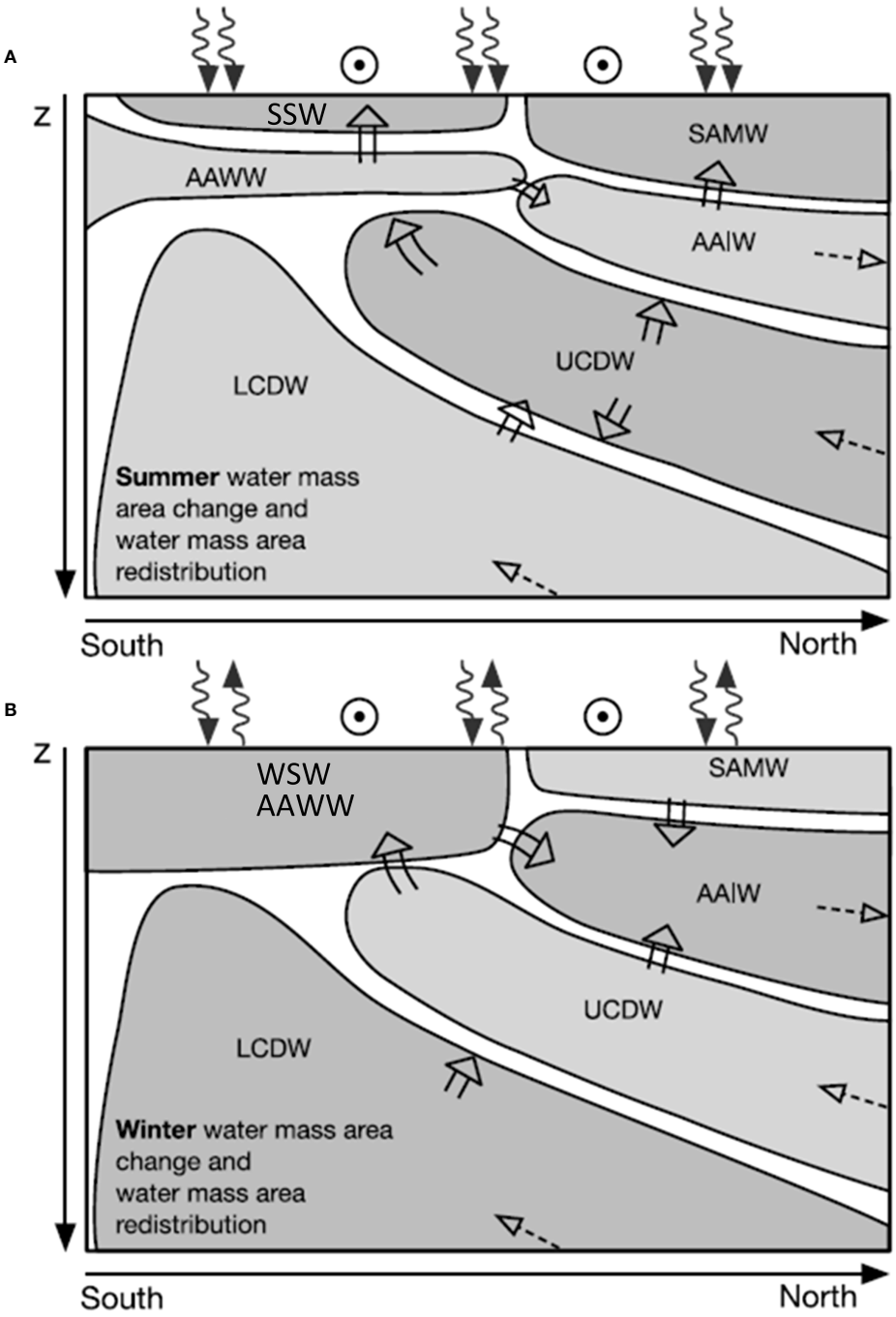

FIGURE 3
Schematic showing the changes in the distributions of water masses during **(A)** summer and **(B)** winter in depth vs. latitude coordinates. The black circles with dots represent the direction of the zonal winds out of the page. SSW, Summer Surface Water; WSW, Winter Surface Water; AAWW, Antarctic Winter Water; SAMW, Subantarctic Mode Water; AAIW, Antarctic Intermediate Water; UCDW/LCDW, Upper/Lower Circumpolar Deep Water. Figure modified from Evans et al. (2014).

winter, with spatial variation of up to 50 μatm in winter. Temporally, summer surface waters pCO_2 ranged from 300 to 370 μatm, which were mostly undersaturated with respect to the atmospheric pCO_2 (366 μatm in 2005); however, most of them became supersaturated in winter. The regions south of the APF experienced the greatest seasonal variation in pCO_2 (~80 μatm).

Figures 5, 6 show the seasonal variation of surface pCO_2 and ΔpCO_2 (sea surface pCO_2 minus atmospheric pCO_2) from R1 to

TABLE 1 Values of absolute salinity (S_A), conservative temperature (T_{cons}), TA, and DIC in each endmember water mass.

	S_A (g kg^{-1})	T_{cons} (°C)	TA (µmol kg^{-1})	DIC (µmol kg^{-1})
AAWW				
value	34.1	-0.67	2301.3	2174.2
n	91	91	37	40
S.D.	0.07	0.58	7.6	17.6
SSW				
value	33.9	2.39	2275.3	2133.8
n	12846	12846	12798	12167
S.D.	0.09	0.80	6.9	12.4
WSW				
value	34.0	-1.33	2279.0	2164.8
n	7102	7102	7091	6573
S.D.	0.10	0.29	7.8	10.0
UCDW				
value	34.7	1.91	2335.1	2249.5
n	92	92	32	44
S.D.	0.08	0.23	9.2	8.9

The surface waters were defined as depths shallower than 30 m. The values for surface endmembers SSW and WSW were determined from the DPT dataset, and the values for subsurface endmembers AAWW and UCDW were determined from the GLODAPv2 dataset, with depth profiles from cruises in March 2006, February 2009, and September 2009, respectively.

R4. Overall, the region acts as a weak sink of CO_2 from the atmosphere (Fig. 6E), with R1 and R2 being a near neutral region (winter CO_2 source counteracted by summer sink), and R3 and R4 being a sink region (persistent CO_2 sink except for a couple of months). The maxima of surface ocean pCO_2 were often reached in austral winter, when upward transport of deep water brings CO_2-rich water to the surface, and the minima were mostly observed in summer, when biological production draws down the surface CO_2 level (Takahashi et al., 2009). The seasonal amplitude of ΔpCO_2 is generally less than 10 µatm throughout Drake Passage (Figures 6A–D), in agreement with the comprehensive study of surface pCO_2 in Drake Passage carried out by Fay et al. (2018) and Munro et al. (2015b).

3.2 Comparisons between ship- and float-based carbonate parameters

We constrained the 8 floats within R1-R4 regions. For comparison between different sampling years, both the ship-based and float-based pCO_2 were adjusted to the reference year 2005 according to the reported rates of anthropogenic change in the Southern Ocean (see Section 2.3.1). Since the Argo float collected data from surface to deep (2000 m) during a 10-day cycle, it happened that most of the data located in R4, and most of them were collected in winter. Significant disagreement between the ship- and float-based pCO_2 and ΔpCO_2 were found in R4 (Figures 4–6).

In R4, float-based pCO_2 and ΔpCO_2 were significantly higher than ship-based except for a couple of months (November and December). Since the atmospheric pCO_2 is rather stable in the southern hemisphere, the deviations in pCO_2 are therefore equivalent to deviations in ΔpCO_2. Such deviations (float minus ship) seem to be consistent through February to September, ranging from 6 to 24 µatm (averaged 14 µatm), with largest deviations in autumn and winter (May to August). This suggests a possible overestimation of pCO_2 and ΔpCO_2 by float-based observations. In terms of pCO_2, this overestimation means 2-6% uncertainty (6-24 µatm divided by mean pCO_2 of 363 µatm); however, in terms of ΔpCO_2, this would mean 100-400% uncertainty (6-24 µatm divided by mean of absolute ΔpCO_2 value of 6 µatm).

4 Discussion

4.1 The theoretical envelope of upwelling-induced pCO_2

Tracer values from Table 1 were applied to Equations 1-2 to estimate the fractions of AAWW and SSW present in surface water. DIC is conservative regarding the mixing process but affected by biogeochemical processes, therefore we calculated (using Equation 2) the concentrations of 'mixed' DIC in WSW just from mixing of AAWW and SSW DIC values; pCO_2 is not conservative regarding the mixing process, the values of 'mixed' pCO_2 in WSW were therefore calculated from the carbonate system with the inputs of 'mixed' TA and 'mixed' DIC, using CO_2SYS (Van Heuven et al., 2011). The choice of dissociation constants was following the global scale studies such as Wu et al. (2019).

Using TA as tracer resulted in calculated fractions of AAWW=13% and SSW=87% (fraction uncertainty of 20%), and subsequent mixed DIC of 2139 ± 13 µmol kg^{-1} and pCO_2 = 307 ± 27 µatm, both of which are less than the observed levels in the WSW and atmosphere. Using salinity as tracer resulted in calculated fractions of AAWW = 48% (more upwelled waters than TA-derived) and SSW = 52% (fraction uncertainty of 24%), and subsequent mixed DIC of 2153 ± 15 µmol kg^{-1} and pCO_2 = 337 ± 22 µatm, still less than the observed levels in the WSW and atmosphere.

Moreover, even if we accounted for the mixture between UCDW, AAWW, and SSW to form WSW, the results still yielded lower pCO_2 ('mixed' pCO_2 ranged between 310 ± 30 and 330 ± 34 µatm, with UCDW fraction ranging from 6 ± 10% to 14 ± 10% depending on different tracers) than the atmospheric level. Although it seems counterintuitive because UCDW endmember could provide enormous natural carbon to the surface ocean (DeVries et al., 2017), the mixed pCO_2 would be as low as calculated because of the countering effect from high upwelled TA (Wu et al., 2019; Chen et al., 2022).

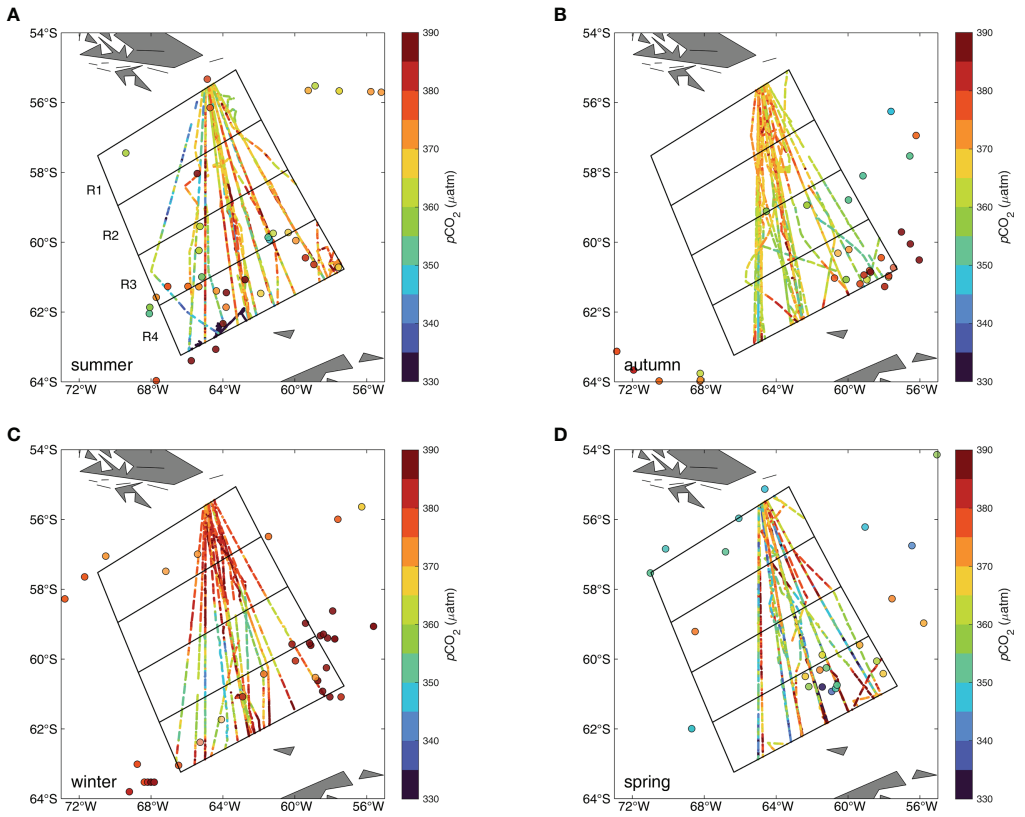

FIGURE 4
The spatial distribution of ship-based and float-based pCO_2 in each season in the surface Drake Passage. **(A–D)** spring to winter. pCO_2 was normalized to year 2005.

Despite that the estimated surface pCO_2 from winter entrainment and upwelling exhibited deviations between different choice of tracers, they served as sensitivity test to each other and both suggested much lower levels of pCO_2 than atmospheric level. The physically 'mixed' pCO_2 was therefore not capable of inducing strong CO_2 outgassing (consistent with Figure 5); R4 thus remained a CO_2 sink region, which also agrees well with a previous assessment that Drake Passage is overall a persistent CO_2 sink in all regions (Munro et al., 2015b; Fay et al., 2018).

4.2 Is the strong winter CO_2 source plausible?

Our results imply that Drake Passage is a weak oceanic sink for CO_2 (Figure 6) and challenge the finding from SOCCOM float data that high-latitude Southern Ocean releases substantial CO_2 (Williams et al., 2017; Gray et al., 2018; Bushinsky et al., 2019). Both approaches used in this study suggest that it is implausible that winter entrainment/upwelling of deep waters into Drake Passage surface layer could produce a magnitude in ΔpCO_2 of as large as 40 μatm (which was suggested by float estimations; Williams et al., 2017) or a remarkable natural CO_2 outgassing signal (Bushinsky et al., 2019). The upwelling of high pCO_2 subsurface waters is therefore limited in causing large winter outgassing from just beneath the surface mixed layer in Drake Passage of the high-latitude Southern Ocean. Although we did not extend our approach to the wider Southern Ocean due to the lack of ship-based data that prohibited the constructions of surface carbon balance calculation, we presume that the proposed theoretical framework for Drake Passage would also work for the Indo-Pacific sector which are hot spots for upwelling of natural CO_2 from Indo-Pacific Deep Water (Chen et al., 2022; Prend et al., 2022). It is reasonable that some discrepancies between ship- and float-derive pCO_2 could be attributed to episodic or short-term (weekly to monthly) variabilities during the float observation (e.g., storms and mesoscale events) which would cause peaks in pCO_2 (Kwak et al., 2021; Nicholson et al., 2022). However, our study reveals that the inconsistency existed throughout the observation on a longer timescale (yearly; Figure 6D). Furthermore, our study is also in line with some other studies applying novel techniques (Long et al., 2021; Mackay & Watson, 2021; Sutton et al., 2021;

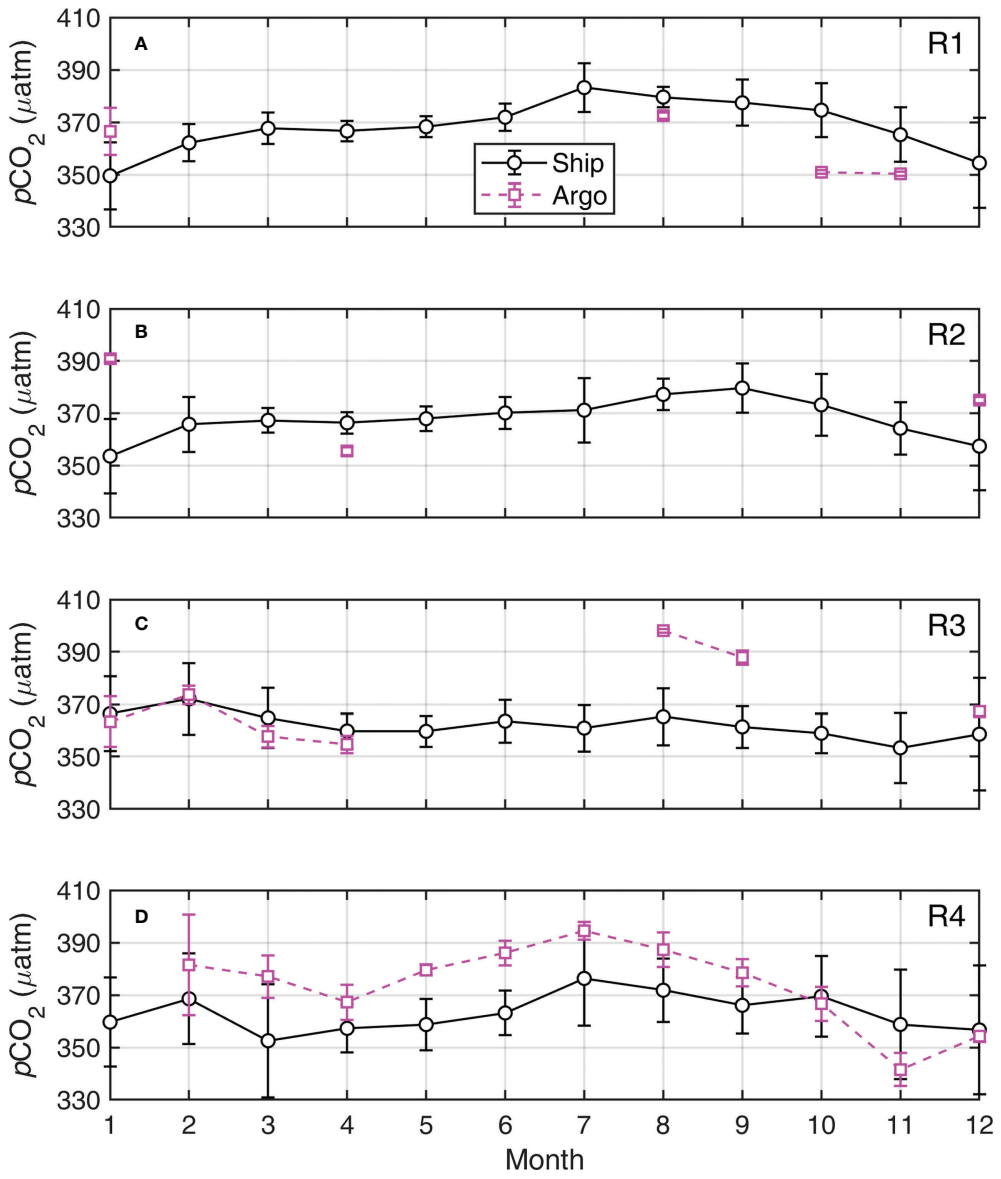

FIGURE 5
The comparison between ship-based and float-based monthly pCO_2 in each region **(A–D)** of the Drake Passage.

Wu et al., 2022) to indicate the possible overestimation of CO_2 outgassing by SOCCOM floats which could be due to erroneous pH measurements or carbonate system-related biases (Álvarez et al., 2020; Wu et al., 2022).

Although it seems contradictory that Fay et al. (2018) and our study have used similar datasets (both used DPT and SOCCOM datasets) but came to different conclusions regarding the consistency between ship- and float-based pCO_2 (Fay et al. claimed that the float-based pCO_2 fall within the range of ship-based values given the uncertainty on the estimates), their study indeed revealed the overall higher float-based pCO_2 than ship-based, particularly in winter, which is consistent with our findings. Fay et al. (2018) showed in their crossover analysis between ship- and float-based pCO_2 in their Figure 9B equally large discrepancies and highly variable difference (i.e., large standard deviation). All of their findings consistently pointed to the fact that bias in float-based pCO_2 is considerable. However, Fay et al. (2018) used a different averaging approach to obtain the final uncertainty value (grey box in their Figure 9B), during which process the overall uncertainty reduced to ±11 μatm, i.e., within the range of observational uncertainties as these authors argue. Noteworthy, ± 11 μatm is

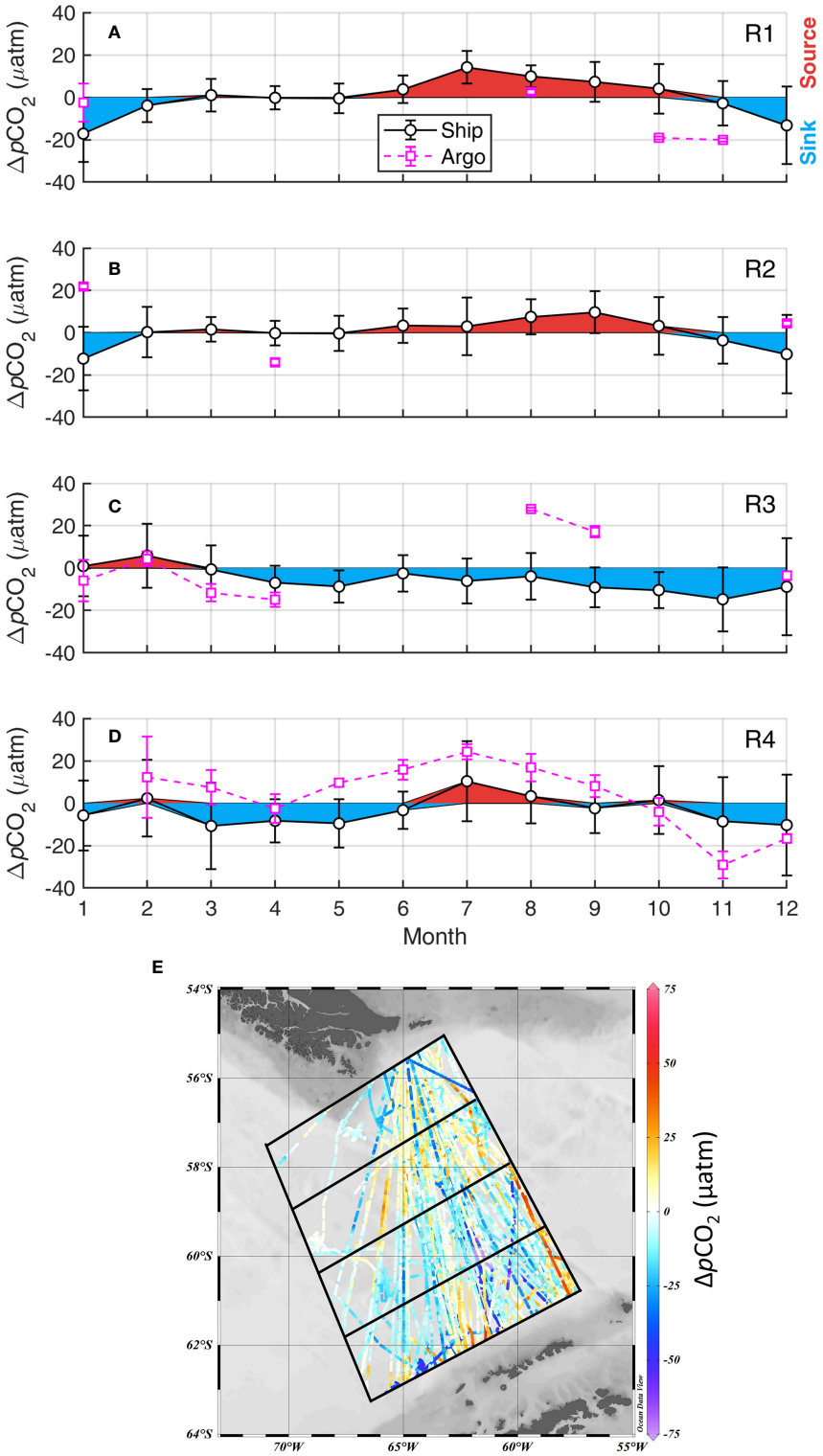

FIGURE 6
The comparison between ship-based and float-based monthly ΔpCO_2 in each region of the Drake Passage. **(A–D)** monthly ΔpCO_2 in different regions from R1 to R4. **(E)** the spatial pattern of ΔpCO_2. ΔpCO_2 means difference between the sea surface and atmospheric pCO_2. The error bars represent the standard deviations of monthly mean values.

by no means an acceptable uncertainty range for the pCO_2 observation, which is five times larger than the typical ship-based pCO_2 uncertainty of ±2 μatm (Pierrot et al., 2009). In all cases, pCO_2 is eventually used to calculate air-sea CO_2 flux based on $F_{CO2} = k \times \alpha \times \Delta pCO_2$, where k is CO_2 gas transfer velocity, α is the CO_2 solubility, and ΔpCO_2 is the difference between sea surface and atmospheric level. Given that atmospheric pCO_2 is stable and can be regarded as a constant at short timescale, the uncertainty of F_{CO2} would largely depend on the uncertainty of ΔpCO_2, in their case this would cause ~180% uncertainty in F_{CO2} estimates and therefore cannot be ignored.

5 Conclusion

The autonomous biogeochemical-Argo floats have collected tremendous invaluable data to understand the global ocean carbon cycle, and made great efforts to fill the data gaps in the highly under-sampled Southern Ocean. Since the first few carbonate system studies from the SOCCOM project (Williams et al., 2017; Gray et al., 2018; Bushinsky et al., 2019) that revealed a striking CO_2 outgassing signal due to upwelling in the high-latitude Southern Ocean (particularly in winter), there has been debates on the float-based data quality and the magnitude of float-derived Southern Ocean CO_2 flux (e.g., Álvarez et al., 2020; Long et al., 2021; Mackay & Watson, 2021; Sutton et al., 2021; Wu et al., 2022). In this study, we chose the Drake Passage as a window of research to address the above issues, because it has been extensively observed by both ships and floats. We collected all ship-based pCO_2 observations in Drake Passage during 2002-2017 and compared them with 8 series of float-based observations in the same region during 2014-2020. The detrended ship- and float-based pCO_2 showed similar spatiotemporal patterns, however, a discrepancy of 14 μatm (float > ship) was found. We further applied an independent approach based on surface carbon balance to estimate the theoretical value of surface pCO_2 if it was enhanced by upwelling, and suggested that upwelling is insufficient to cause the above discrepancy. These findings are against the previous statements (e.g., Fay et al., 2018) that float-based pCO_2 fall within the range of ship-based values given the uncertainty on the estimates, although we both have found comparable deviations (averaged 14 μatm, with maximum of 24 μatm) to theirs (averaged 11 μatm, with maximum of 25 μatm). This is because the way that Fay et al. (2018) reported their results was based on relative uncertainty, therefore an uncertainty in pCO_2 ± 2.7% (equivalent to ±11 μatm) would sound reasonable, although ±11 μatm is already five times larger than the general ship-based pCO_2 uncertainty. We argue that more cautions have to be made in reporting/estimating the uncertainty, because essentially the ±2.7% pCO_2 uncertainty would mean ~180% uncertainty in CO_2 flux estimates.

Data availability statement

Publicly available datasets were analyzed in this study. This data can be found here: https://www.ldeo.columbia.edu/res/pi/CO2/; https://soccom.princeton.edu/.

Author contributions

Conceptualization, YW. Methodology, YW. Software, YW. Validation, DQ. Writing—original draft preparation, YW. Writing—review and editing, YW and DQ. All authors have read and agreed to the published version of the manuscript.

Funding

This study was funded by the Independent Research Projects of Southern Marine Science and Engineering Guangdong Laboratory (Zhuhai) (SML2021SP306), National Key Research and Development Program of China (2019YFE0114800, 2019YFC1509101), National Natural Science Foundation of China (42106222), Natural Science Foundation of Fujian Province, China (2020J05075, 2019J05148), and the Scientific Research Foundation of Ministry of Natural Resources (2019032).

Acknowledgments

We acknowledge the work by the data providers and scientists carrying out data collection, quality-control, and synthesis that led to the production of the datasets used here. We also sincerely thank the two reviewers for their constructive suggestions and comments.

Conflict of interest

The authors declare that the research was conducted in the absence of any commercial or financial relationships that could be construed as a potential conflict of interest.

Publisher's note

References

Álvarez, M., Fajar, N. M., Carter, B. R., Guallart, E. F., Pérez, F. F., Woosley, R. J., et al. (2020). Global ocean spectrophotometric pH assessment: consistent inconsistencies. *Environ. Sci. Technol.* 54 (18), 10977–10988. doi: 10.1021/acs.est.9b06932

Bakker, D. C. E., Pfeil, B., Landa, C. S., Metzl, N., O'Brien, K. M., Olsen, A., et al. (2016). A multi-decade record of high-quality fCO2 data in version 3 of the surface ocean CO2 atlas (SOCAT). *Earth System Sci. Data* 8 (2), 383–413. doi: 10.5194/essd-8-383-2016

Brown, M. S., Munro, D. R., Feehan, C. J., Sweeney, C., Ducklow, H. W., and Schofield, O. M. (2019). Enhanced oceanic CO2 uptake along the rapidly changing West Antarctic peninsula. *Nat. Climate Change* 9 (9), 678–683. doi: 10.1038/s41558-019-0552-3

Bushinsky, S. M., Landschutzer, P., Rodenbeck, C., Gray, A. R., Baker, D., Mazloff, M. R., et al. (2019). Reassessing southern ocean air-sea CO2 flux estimates with the addition of biogeochemical float observations. *Global Biogeochem. Cycles* 33 (11), 1370–1388. doi: 10.1029/2019GB006176

Carter, B. R., Feely, R. A., Williams, N. L., Dickson, A. G., Fong, M. B., and Takeshita, Y. (2018). Updated methods for global locally interpolated estimation of alkalinity, pH, and nitrate. *Limnol. Oceanog.: Methods* 16 (2), 119–131. doi: 10.1002/lom3.10232

Chapman, C. C., Lea, M.-A., Meyer, A., Sallée, J.-B., and Hindell, M. (2020). Defining southern ocean fronts and their influence on biological and physical processes in a changing climate. *Nat. Climate Change* 10 (3), 209–219. doi: 10.1038/s41558-020-0705-4

Chen, H., Haumann, F. A., Talley, L. D., Johnson, K. S., and Sarmiento, J. L. (2022). The deep ocean's carbon exhaust. *Global Biogeochem. Cycles* 36, e2021GB007156. doi: 10.1029/2021GB007156

DeVries, T. (2014). The oceanic anthropogenic CO2 sink: Storage, air-sea fluxes, and transports over the industrial era. *Global Biogeochem. Cycles* 28 (7), 631–647. doi: 10.1002/2013gb004739

DeVries, T., Holzer, M., and Primeau, F. (2017). Recent increase in oceanic carbon uptake driven by weaker upper-ocean overturning. *Nature* 542 (7640), 215–218. doi: 10.1038/nature21068

Evans, D. G., Zika, J. D., Naveira Garabato, A. C., and Nurser, A. J. G. (2014). The imprint of southern ocean overturning on seasonal water mass variability in drake passage. *J. Geophys. Research: Oceans* 119 (11), 7987–8010. doi: 10.1002/2014JC010097

Fay, A. R., Lovenduski, N. S., McKinley, G. A., Munro, D. R., Sweeney, C., Gray, A. R., et al. (2018). Utilizing the drake passage time-series to understand variability and change in subpolar southern ocean pCO_2. *Biogeosciences* 15 (12), 3841–3855. doi: 10.5194/bg-15-3841-2018

Friedlingstein, P., Jones, M. W., O'Sullivan, M., Andrew, R. M., Bakker, D. C. E., Hauck, J., et al. (2022). Global carbon budget 2021. *Earth Syst. Sci. Data* 14 (4), 1917–2005. doi: 10.5194/essd-14-1917-2022

Gray, A. R., Johnson, K. S., Bushinsky, S. M., Riser, S. C., Russell, J. L., Talley, L. D., et al. (2018). Autonomous biogeochemical floats detect significant carbon dioxide outgassing in the high-latitude southern ocean. *Geophys. Res. Lett.* 45 (17), 9049–9057. doi: 10.1029/2018GL078013

Gruber, N., Clement, D., Carter, B. R., Feely, R. A., van Heuven, S., Hoppema, M., et al. (2019a). The oceanic sink for anthropogenic CO2 from 1994 to 2007. *Science* 363 (6432), 1193–1199. doi: 10.1126/science.aau5153

Gruber, N., Gloor, M., Mikaloff Fletcher, S. E., Doney, S. C., Dutkiewicz, S., Follows, M. J., et al. (2009). Oceanic sources, sinks, and transport of atmospheric CO2. *Global Biogeochem. Cycles* 23 (1), GB1005. doi: 10.1029/2008GB003349

Gruber, N., Landschützer, P., and Lovenduski, N. S. (2019b). The variable southern ocean carbon sink. *Ann. Rev. Mar. Sci.* 11 (1), 159–186. doi: 10.1146/annurev-marine-121916-063407

Johnson, K. S., Plant, J. N., Coletti, L. J., Jannasch, H. W., Sakamoto, C. M., Riser, S. C., et al. (2017). Biogeochemical sensor performance in the SOCCOM profiling float array. *J. Geophys. Research: Oceans* 122 (8), 6416–6436. doi: 10.1002/2017JC012838

Kwak, K., Song, H., Marshall, J., Seo, H., and McGillicuddy,D. J. Jr. (2021). Suppressed pCO_2 in the Southern Ocean due to the interaction between current and wind. *Journal of Geophysical Research: Oceans*, 126, e2021JC017884. doi: 10.1029/2021JC017884

Landschützer, P., Gruber, N., Bakker, D., and Schuster, U. (2014). Recent variability of the global ocean carbon sink. *Global Biogeochem. Cycles* 28 (9), 927–949. doi: 10.1002/2014GB004853

Landschützer, P., Gruber, N., Haumann, F. A., Rödenbeck, C., Bakker, D. C. E., van Heuven, S., et al. (2015). The reinvigoration of the southern ocean carbon sink. *Science* 349 (6253), 1221–1224. doi: 10.1126/science.aab2620

Le Quéré, C., Rödenbeck, C., Buitenhuis, E. T., Conway, T. J., Langenfelds, R., Gomez, A., et al. (2007). Saturation of the southern ocean CO2 sink due to recent climate change. *Science* 316 (5832), 1735–1738. doi: 10.1126/science.1136188

Long, M. C., Stephens, B. B., McKain, K., Sweeney, C., Keeling, R. F., Kort, E. A., et al. (2021). Strong southern ocean carbon uptake evident in airborne observations. *Science* 374 (6572), 1275–1280. doi: 10.1126/science.abi4355

Lovenduski, N. S., Gruber, N., and Doney, S. C. (2008). Toward a mechanistic understanding of the decadal trends in the southern ocean carbon sink. *Global Biogeochem. Cycles* 22 (3), GB3016. doi: 10.1029/2007gb003139

Lovenduski, N. S., Gruber, N., Doney, S. C., and Lima, I. D. (2007). Enhanced CO2 outgassing in the southern ocean from a positive phase of the southern annular mode. *Global Biogeochem. Cycles* 21 (2), GB2026. doi: 10.1029/2006gb002900

Lumpkin, R., and Speer, K. (2007). Global ocean meridional overturning. *J. Phys. Oceanog.* 37 (10), 2550–2562. doi: 10.1175/JPO3130.1

Mackay, N., and Watson, A. (2021). Winter air-sea CO2 fluxes constructed from summer observations of the polar southern ocean suggest weak outgassing. *J. Geophys. Research: Oceans* 126, e2020JC016600. doi: 10.1029/2020JC016600

Marshall, J., and Speer, K. (2012). Closure of the meridional overturning circulation through southern ocean upwelling. *Nat. Geosci.* 5 (3), 171–180. doi: 10.1038/ngeo1391

Mikaloff Fletcher, S. E., Gruber, N., Jacobson, A. R., Doney, S. C., Dutkiewicz, S., Gerber, M., et al. (2006). Inverse estimates of anthropogenic CO2 uptake, transport, and storage by the ocean. *Global Biogeochem. Cycles* 20 (2), GB2002. doi: 10.1029/2005gb002530

Munro, D. R., Lovenduski, N. S., Stephens, B. B., Newberger, T., Arrigo, K. R., Takahashi, T., et al. (2015a). Estimates of net community production in the southern ocean determined from time series observations (2002–2011) of nutrients, dissolved inorganic carbon, and surface ocean pCO_2 in drake passage. *Deep Sea Res. Part II: Topical Stud. Oceanog.* 114, 49–63. doi: 10.1016/j.dsr2.2014.12.014

Munro, D. R., Lovenduski, N. S., Takahashi, T., Stephens, B. B., Newberger, T., and Sweeney, C. (2015b). Recent evidence for a strengthening CO_2 sink in the southern ocean from carbonate system measurements in the drake passage (2002–2015). *Geophys. Res. Lett.* 42 (18), 7623–7630. doi: 10.1002/2015GL065194

Nicholson, S.-A., Whitt, D. B., Fer, I., du Plessis, M. D., Lebéhot, A. D., Swart, S., and Monteiro, P. M.S. (2022). Storms drive outgassing of CO2 in the subpolar Southern Ocean. *Nature Communications*, 13(1), 158. doi: 10.1038/s41467-021-27780-w

Olsen, A., Lange, N., Key, R. M., Tanhua, T., Bittig, H. C., Kozyr, A., et al. (2020). An updated version of the global interior ocean biogeochemical data product, GLODAPv2.2020. *Earth System Sci. Data* 12 (4), 3653–3678. doi: 10.5194/essd-12-3653-2020

Orsi, A. H., Whitworth, T., and Nowlin, W. D. (1995). On the meridional extent and fronts of the Antarctic circumpolar current. *Deep Sea Res. Part I: Oceanographic Res. Papers* 42 (5), 641–673. doi: 10.1016/0967-0637(95)00021-W

Pierrot, D., Neill, C., Sullivan, K., Castle, R., Wanninkhof, R., Lüger, H., et al. (2009). Recommendations for autonomous underway pCO_2 measuring systems and data-reduction routines. *Deep Sea Res. Part II: Topical Stud. Oceanog.* 56 (8-10), 512–522. doi: 10.1016/j.dsr2.2008.12.005

Prend, C. J., Gray, A. R., Talley, L. D., Gille, S. T., Haumann, F. A., Johnson, K. S., et al. (2022). Indo-pacific sector dominates southern ocean carbon outgassing. *Global Biogeochem. Cycles* 36, e2021GB007226. doi: 10.1029/2021GB007226

Sarmiento, J. L., Gruber, N., Brzezinski, M. A., and Dunne, J. P. (2004). High-latitude controls of thermocline nutrients and low latitude biological productivity. *Nature* 427 (6969), 56–60. doi: 10.1038/nature02127

Sarmiento, J. L., and Toggweiler, J. R. (1984). A new model for the role of the oceans in determining atmospheric pCO_2. *Nature* 308 (5960), 621–624. doi: 10.1038/308621a0

Sprintall, J., Chereskin, T. K., and Sweeney, C. (2012). High-resolution underway upper ocean and surface atmospheric observations in drake passage: Synergistic measurements for climate science. *Oceanography* 25 (3), 70–81. doi: 10.5670/oceanog.2012.77

Sutton, A. J., Williams, N. L., and Tilbrook, B. (2021). Constraining southern ocean CO2 flux uncertainty using uncrewed surface vehicle observations. *Geophys. Res. Lett.* 48 (3), e2020GL091748. doi: 10.1029/2020GL091748

Takahashi, T., Sutherland, S. C., Chipman, D. W., Goddard, J. G., Ho, C., Newberger, T., et al. (2014). Climatological distributions of pH, pCO_2, total CO_2, alkalinity, and CaCO3 saturation in the global surface ocean, and temporal changes at selected locations. *Mar. Chem.* 164 (0), 95–125. doi: 10.1016/j.marchem.2014.06.004

Takahashi, T., Sutherland, S. C., Wanninkhof, R., Sweeney, C., Feely, R. A., Chipman, D. W., et al. (2009). Climatological mean and decadal change in surface ocean pCO_2, and net sea–air CO2 flux over the global oceans. *Deep Sea Res. II* 56 (8), 554–577. doi: 10.1016/j.dsr2.2008.12.009

Takeshita, Y., Johnson, K. S., Martz, T. R., Plant, J. N., and Sarmiento, J. L. (2018). Assessment of autonomous pH measurements for determining surface seawater partial pressure of CO2. *J. Geophys. Research: Oceans* 123 (6), 4003–4013. doi: 10.1029/2017JC013387

Talley, L. D. (2013). Closure of the global overturning circulation through the Indian, pacific, and southern oceans: Schematics and transports. *Oceanography* 26 (1), 80–97. doi: 10.5670/oceanog.2013.07

Thorpe, S. E., Heywood, K. J., Brandon, M. A., and Stevens, D. P. (2002). Variability of the southern Antarctic circumpolar current front north of south Georgia. *J. Mar. Syst.* 37 (1), 87–105. doi: 10.1016/S0924-7963(02)00197-5

Van Heuven, S., Pierrot, D., Rae, J. W. B., Lewis, E., and Wallace, D. W. R. (2011). MATLAB program developed for CO_2 system calculations. Carbon Dioxide Information Analysis Center, Oak Ridge National Laboratory, U.S. Department of Energy, Oak Ridge, Tennessee. doi: 10.3334/CDIAC/otg.CO2SYS_MATLAB_v1.1

Williams, N. L., Juranek, L. W., Feely, R. A., Johnson, K. S., Sarmiento, J. L., Talley, L. D., et al. (2017). Calculating surface ocean pCO_2 from biogeochemical argo floats equipped with pH: An uncertainty analysis. *Global Biogeochem. Cycles* 31 (3), 591–604. doi: 10.1002/2016GB005541

Williams, N. L., Juranek, L. W., Johnson, K. S., Feely, R. A., Riser, S. C., Talley, L. D., et al. (2016). Empirical algorithms to estimate water column pH in the southern ocean. *Geophys. Res. Lett.* 43 (7), 3415–3422. doi: 10.1002/2016GL068539

Wu, Y., Bakker, D. C. E., Achterberg, E. P., Silva, A. N., Pickup, D. D., Li, X., et al. (2022). Integrated analysis of carbon dioxide and oxygen concentrations as a quality control of ocean float data. *Commun. Earth Environ.* 3 (1), 92. doi: 10.1038/s43247-022-00421-w

Wu, Y., Hain, M. P., Humphreys, M. P., Hartman, S., and Tyrrell, T. (2019). What drives the latitudinal gradient in open-ocean surface dissolved inorganic carbon concentration? *Biogeosciences* 16 (13), 2661–2681. doi: 10.5194/bg-16-2661-2019